



Rapidly oscillating ac-driven long Josephson junctions with phase-shifts

Amir Ali¹, Hadi Susanto^{*}, Jonathan A.D. Wattis

School of Mathematical Sciences, University of Nottingham, University Park, Nottingham NG7 2RD, UK

ARTICLE INFO

Article history:

Received 20 June 2012

Received in revised form

1 October 2012

Accepted 4 December 2012

Available online 11 December 2012

Communicated by S. Kai

Keywords:

Josephson junction

Rapidly oscillating drive

Fractional fluxon

Averaging method

ABSTRACT

A long Josephson junction containing regions with phase shifts driven by a rapidly-oscillating ac-drive is considered. An average equation, based on multiple time scale analysis is derived, which is effectively a double sine-Gordon equation. In the presence of internal phase-shifts, it is analytically shown through the average equation that the ac-drive can influence the type of the ground state. In particular, the cases of $0 - \kappa$ and $0 - \pi - 0$ junctions are considered. For the $0 - \kappa$ junction it is shown that an external ac-drive can *reduce* the critical bias current above which the junction switches to the resistive state. As for the $0 - \pi - 0$ junction an ac-drive is shown to *increase* the critical length above which the ground state is nonuniform. Numerical comparisons are performed, and good agreement is obtained.

© 2012 Elsevier B.V. All rights reserved.

1. Introduction

A Josephson junction is an electronic circuit consisting of two superconductors connected by a thin non-superconducting layer, and is the basis of a large number of developments both in fundamental research and in application to electronic devices [1]. Even though there is no applied voltage difference, a flow of electrons can tunnel from one superconductor to the other due to the overlapping quantum mechanical waves in the two superconductors of the Josephson junction. If we denote the difference in phases of the wave functions by ϕ and the spatial and temporal variable along the junction by x and t , respectively, the electron flow tunnelling across the barrier, i.e. the Josephson current, I is proportional to the sine of $\phi(x, t)$. In a lossless and undriven long Josephson junction, the phase difference ϕ satisfies the sine-Gordon equation.

A particular solution of the sine-Gordon equation is a kink solution, which is a topological soliton. The solution represents a twist in the variable ϕ which takes the system from one solution $\phi = 0$ to an adjacent one with $\phi = 2\pi$. In the context of long Josephson junctions, this kink corresponds to a vortex of supercurrent, which can be formed inside the Josephson barrier. The supercurrents circulate around the vortex's centre and carry a magnetic field with the total flux equal to a single flux quantum

$\Phi_0 \approx 2.07 \times 10^{-15}$ Wb. Therefore, such a vortex is also referred to as a (Josephson) fluxon.

One of the important properties of Josephson junctions is their behaviour when radiated with external radio-frequency (rf) microwave fields [2,3]. This can be modelled by a sine-Gordon equation driven with a periodic (ac) force. In particular, interactions of fluxons in long Josephson junctions and ac-drives may yield rich dynamics, including oscillatory and effectively progressive motions of fluxons (see, e.g., [4–6] and references therein). Microwave driven Josephson junctions have also been used to study this ratchet effect, that is, the unidirectional motion under the influence of a force with zero mean [7,8]. When the driving frequency and amplitude of the applied microwave are larger than the Josephson plasma frequency ω_p , one may also obtain unstable, but long-lived half-fluxons (π -kinks), which are not present in the undriven system [9,10].

Recently, the study of the effects of microwave field radiation has been extended both experimentally and theoretically to the so-called Josephson junctions with phase shifts [11–14]. Such junctions were first proposed by Bulaevskii et al. [15,16]. A non-trivial ground-state can be realized in the junctions, characterized by the spontaneous generation of a fractional fluxon, i.e. a vortex carrying a fraction of magnetic flux quantum. This remarkable property can be invoked by intrinsically building piecewise constant phase-shifts $\theta(x)$ into the junction. Due to the phase-shift, the supercurrent relation becomes $I \sim \sin(\phi + \theta)$. Presently, one can impose phase-shifts in long Josephson junctions using several methods, such as by installing magnetic impurities [17] or Abrikosov vortices [18], using multilayer junctions with controlled thicknesses over the ferromagnetic barrier [19], pairs of current injectors [20] and junctions with unconventional order parameter symmetry [21–23]. When radiated with magnetic

^{*} Corresponding author. Tel.: +44 115 951 3896; fax: +44 115 951 4951.

E-mail address: hadi.susanto@nottingham.ac.uk (H. Susanto).

¹ On leave from Department of Mathematics, University of Malakand, Chakdara, K. Pukhtoonkhwa, Pakistan.

fields, such novel types of junctions exhibit interesting dynamics, such as half-integer Shapiro steps [11] and different characteristics of self-resonance modes known as Fiske modes [24]. As the aforementioned works were concentrated on the *dynamics* of the junctions, in this paper we consider for the first time the influence of high-frequency radiation fields to the existence of ‘time-averagely’ *static* ground states of the junctions.

The dynamics of the phase difference ϕ of a Josephson junction with phase-shifts is modelled by the perturbed sine-Gordon equation

$$\phi_{tt}(x, t) - \phi_{xx}(x, t) + \sin(\phi + \theta) = \gamma - \alpha\phi_t + f \cos(\Omega t). \quad (1)$$

Eq. (1) is dimensionless, x and t are normalized to the Josephson penetration length λ_J and the inverse plasma frequency ω_p^{-1} , respectively, and α is the damping coefficient due to electron tunnelling across the junction. The parameter γ represents an applied (dc) bias current. The applied time periodic (ac) drive is represented by the final term of the governing equation above. Because of the nondimensionalization of the temporal variable t , the Josephson plasma frequency ω_p corresponds to $\Omega = 1$. Here, we consider the experimentally relevant case $\Omega \gg 1$. The case $\Omega < 1$ has been considered theoretically in [25] (see also [12,13] for the experiments). In this paper, we consider two particular configurations of phase shift, namely

$$\theta(x) = \begin{cases} 0, & |x| > a, \\ \pi, & |x| < a, \end{cases} \quad (2)$$

and

$$\theta(x) = \begin{cases} 0, & x < 0, \\ -\kappa, & x > 0, \end{cases} \quad (3)$$

which are referred to as the $0-\pi-0$ and $0-\kappa$ Josephson junctions, respectively. The phase field ϕ is then naturally subject to the continuity conditions at the position of the jump in the Josephson phase (the discontinuity), i.e.

$$\phi(\pm a^-) = \phi(\pm a^+), \quad \phi_x(\pm a^-) = \phi_x(\pm a^+), \quad (4)$$

for the $0-\pi-0$ junction and

$$\phi(0^-) = \phi(0^+), \quad \phi_x(0^-) = \phi_x(0^+), \quad (5)$$

for the $0-\kappa$ junction. The quantity ϕ_{xx} may be discontinuous at the points where θ is discontinuous.

The unperturbed $0-\pi-0$ junction, i.e. (1) and (2) with $\gamma = f = 0$, has

$$\phi_0(x, t) = 0, \quad (6)$$

(mod 2π) as the ground state. Studying the stability of the constant solution, one finds there is a critical facet length $a_c = \pi/4$ above which the solution is unstable and the ground state is spatially nonuniform [26]. The ground state represents a pair of fractional fluxons of opposite polarities. A scanning microscopy image of fractional fluxons can be seen in, e.g., [22,27].

As for the unperturbed $0-\kappa$ junction, i.e. (1) and (3) with $\gamma = f = 0$, the ground state of the system is (mod 2π)

$$\phi_0(x, t) = \begin{cases} 4 \tan^{-1} e^{x_0+x}, & x < 0, \\ \kappa - 4 \tan^{-1} e^{x_0-x}, & x > 0, \end{cases} \quad (7)$$

where $x_0 = \ln \tan(\kappa/8)$. Physically, $\phi_0(x, t)$ (7) represents a fractional fluxon that is spontaneously generated at the discontinuity. In the presence of an applied dc bias current ($\gamma \neq 0$), the fractional fluxon will be deformed. When the current is large enough, the static ground state will cease to exist and the junction switches to a resistive state by alternately releasing travelling fluxons and antifluxons. The minimum current at which the junction switches

to such a state is called the critical current $\gamma_c = 2 \sin(\kappa/2)/\kappa$ [28,29].

When $f \neq 0$, the threshold distance in $0-\pi-0$ junctions and the critical current γ_c in $0-\kappa$ junctions are expected to be different. Here, we show that rapidly oscillating ac-drives will increase the threshold distance in $0-\pi-0$ junctions and decrease the critical current in $0-\kappa$ junctions. This is the main result of the present paper. We derive and study an ‘average’ equation describing the average dynamics of the system. The average equation has the form of a double sine-Gordon equation, and is obtained through the method of averaging. The idea of the method is to determine conditions under which solutions of an autonomous dynamical system can be used to approximate solutions of a more complicated (i.e. non-autonomous) time-varying dynamical system. Here, the method is based on multiple time scales analysis. A double sine-Gordon equation describing the slow-time dynamics of a rapidly driven sine-Gordon equation was obtained previously through restricting the phase ϕ to Fourier series expansion [30,31] and the normal form technique [9]. In the normal form technique, several canonical transformations are applied to the Hamiltonian system to move mean-zero terms to higher order [32,33]. In [30,31], Kivshar et al. decompose the phase ϕ into the sum of slowly- and rapidly-varying parts. The method solely use asymptotic expansions rather than averaging over the fast oscillation. In both methods, the coefficients of the double sine-Gordon equation are given in terms of Bessel functions. With the method proposed herein, one has more control on the scales of the driving parameters and the coefficients of the ‘average’ equation are given by simple explicit functions, which will be shown later to be a series expansion of the coefficients obtained in [9,30,31]. This is another result of the paper.

The present work is organized as follows. In Section 2, we derive the average equation that represents the slowly-varying dynamics of the phase due to direct ac driving. In Section 3, we discuss the threshold facet length of $0-\pi-0$ junctions, and the critical bias currents in $0-\kappa$ junctions in the presence of ac-drives, based on our analytical results obtained in Section 2. Numerical results are presented in Section 4. Interestingly, for the critical current in $0-\kappa$ junctions, we show numerically that there is a critical driving amplitude, which is a function of the driving frequency, at which the critical dc current is zero. Finally, Section 5 is devoted to conclusions.

2. Multiscale averaging with large driving amplitude

In this section, we derive an average nonlinear equation to describe the slowly-varying dynamics of the sine-Gordon model (1). Even though in the following we derive an average equation for a general configuration $\theta(x)$, we will see that the phase shift does not play any role in the derivation. We consider a particularly experimentally-relevant case where the ac force is rapidly oscillating, i.e. $\Omega \gg 1$, and define a small parameter $0 < \epsilon = 1/\Omega \ll 1$. In experiments the drive amplitude f can be small or large. Nevertheless, as we will see later and as noted in [30,31] when $f \sim \Omega^2$ or larger the modulation due to the fast oscillating drive will no longer be small. Because of that, we consider a large drive amplitude scaled as

$$f = F/\epsilon^{3/2}, \quad F \sim \mathcal{O}(1), \quad (8)$$

for a reason that it is close to the threshold scaling, but the calculation is relatively simple and tractable. Other scalings, including the experimentally relevant case of small f , can be considered similarly.

Clearly the system (1) not only depends on the $t = \mathcal{O}(1)$ -time scale, but also on the fast time scale $t = \mathcal{O}(\epsilon)$, hence we define a series of time scales

$$T_n = \epsilon^{n/2}t, \quad n = -2, -1, 0, \dots \quad (9)$$

We seek a solution of (1) in terms of the asymptotic expansion

$$\phi(x, t) = \phi_0 + \epsilon^{1/2}\phi_1 + \epsilon\phi_2 + \epsilon^{3/2}\phi_3 + \epsilon^2\phi_4 + \dots, \quad (10)$$

where $\phi_j = \phi_j(x, T_{-2}, T_{-1}, T_0, \dots)$.

It should be noted that $T_{-2} = t/\epsilon$ is the fast variable and it will be shown later that ϕ_0 is independent of T_{-2} . For $0 < \epsilon \ll 1$ the variable T_{-2} changes more rapidly than T_j for $j > -2$, and we can think of $T_j (j > -2)$ as being constant. When considering the problem over the slow time scales, we will assume that the average

$$\langle \phi_i \rangle = \frac{1}{2\pi} \int_0^{2\pi} \phi_i(x, T_{-2}, \dots) dT_{-2} = 0, \quad (11)$$

that is, $\phi_i(x, T_{-2}, T_{-1}, \dots)$, $i = 1, 2, \dots$, have zero mean and are periodic in T_{-2} with period 2π . The assumption (11) is possible because any arbitrary function in ϕ_i that is independent of T_{-2} can be absorbed into ϕ_0 . In this way, $\phi_0(x, T_{-2}, T_{-1}, T_0, \dots)$ represents the average of $\phi(x, t)$ and for that reason the governing equation for ϕ_0 is referred to as the ‘average’ equation.

Denoting $D_n = \partial/\partial T_n$, the multiscale expansion for the time variable implies that the partial derivative becomes

$$\frac{\partial}{\partial t} = \epsilon^{-1}D_{-2} + \epsilon^{-1/2}D_{-1} + D_0 + \epsilon^{1/2}D_1 + \epsilon D_2 + \epsilon^{3/2}D_3 + \epsilon^2D_4 + \dots. \quad (12)$$

Substituting (10) and (12) into (1), expanding and collecting terms in powers of ϵ , one obtains a hierarchy of equations.

Terms of order $\mathcal{O}(\epsilon^{-2})$ give

$$D_{-2}^2\phi_0 = 0, \quad (13)$$

which implies

$$\phi_0(x, T_{-2}, \dots) = C(x, T_{-1}, T_0, \dots)T_{-2} + C_0(x, T_{-1}, T_0, \dots), \quad (14)$$

where C and C_0 are arbitrary at this stage. We set $C(x, T_{-1}, T_0, \dots) = 0$, so that ϕ_0 is periodic in T_{-2} . This shows that the first term in the multiscale expansion is independent of T_{-2} , in other words

$$\phi_0 = \phi_0(x, T_{-1}, T_0, \dots). \quad (15)$$

It can be seen that at the threshold scaling, i.e. when $f \sim 1/\epsilon^2$, the r.h.s. of (13) would not vanish and ϕ_0 would also depend on the fast-time T_{-2} . In that case, the effect of the rapidly oscillating drive is then of order $\mathcal{O}(1)$.

Terms of order $\mathcal{O}(\epsilon^{-3/2})$ give

$$D_{-2}^2\phi_1 + 2D_{-2}D_{-1}\phi_0 = F \cos(T_{-2}). \quad (16)$$

By using the solution (15), we obtain the solution at $\mathcal{O}(\epsilon^{-3/2})$ as

$$\phi_1(x, T_{-2}, T_{-1}, \dots) = -F \cos(T_{-2}) + C_1(x, T_{-1}, T_0, \dots). \quad (17)$$

Here and in the following calculations, we set the unknown function $C_1(x, T_{-1}, T_0, \dots) = 0$ since such a term would make ϕ_1 violate the assumption (11) and in fact, it can be absorbed into ϕ_0 . Hence

$$\phi_1(x, T_{-2}, T_{-1}, \dots) = -F \cos(T_{-2}). \quad (18)$$

The terms of order $\mathcal{O}(\epsilon^{-1})$ give

$$D_{-2}^2\phi_2 + 2D_{-2}D_{-1}\phi_1 + (2D_{-2}D_0 + D_{-1}^2 + \alpha D_{-2})\phi_0 = 0. \quad (19)$$

Since ϕ_1 is independent of T_{-1} and ϕ_0 is independent of T_{-2} , the above equation can be simplified to

$$D_{-2}^2\phi_2 + D_{-1}^2\phi_0 = 0. \quad (20)$$

To obtain a bounded ϕ_2 , it is clear that one must set

$$D_{-1}^2\phi_0 = 0, \quad (21)$$

which implies that ϕ_0 is independent of T_{-1} . Thus, we conclude from (15) and (21) that

$$\phi_0 = \phi_0(x, T_0, T_1, \dots). \quad (22)$$

and

$$\phi_2(x, T_{-2}, T_{-1}, \dots) = 0. \quad (23)$$

Note that condition (21) can also be obtained from the Fredholm alternative. At any order of the expansion, the equation we obtain is always of the form $\mathcal{L}\psi(T_{-2}) = g(T_{-2})$ where $\mathcal{L} = D_{-2}^2$ is clearly a self-adjoint operator and $g : \mathbb{T} \rightarrow \mathbb{R}$ is a smooth 2π -periodic function, with \mathbb{T} being the circle of length 2π . Let $L^2(\mathbb{T})$ be the Hilbert space of 2π -periodic, real-valued functions with inner product

$$\langle y(T_{-2}), z(T_{-2}) \rangle = \int_{\mathbb{T}} y(T_{-2})z(T_{-2}) dT_{-2}. \quad (24)$$

The Fredholm theorem states that the necessary and sufficient condition for the inhomogeneous equation $\mathcal{L}\psi = g$ to have a bounded solution is that $g(T_{-2})$ be orthogonal to the null-space of the operator \mathcal{L} . In $L^2(\mathbb{T})$ the null-space is clearly spanned by a (normalized) constant solution $\psi = 1$. Hence, the solvability condition provided by the Fredholm theorem is

$$\int_0^{2\pi} g(T_{-2}) dT_{-2} = 0. \quad (25)$$

This condition is what we refer to as the solvability condition in the following calculations.

From the terms of order $\mathcal{O}(\epsilon^{-1/2})$, we obtain

$$D_{-2}^2\phi_3 + \alpha D_{-2}\phi_1 = 0, \quad (26)$$

which can be integrated to

$$\phi_3(x, T_{-2}, T_{-1}, \dots) = \alpha F \sin(T_{-2}). \quad (27)$$

The terms of order $\mathcal{O}(1)$ give

$$D_{-2}^2\phi_4 - \phi_{0,xx} + D_0^2\phi_0 + \alpha D_0\phi_0 + \sin(\phi_0 + \theta) - \gamma = 0. \quad (28)$$

Averaging over the fast-time scale, we obtain the solvability condition

$$-\phi_{0,xx} + D_0^2\phi_0 + \alpha D_0\phi_0 + \sin(\phi_0 + \theta) - \gamma = 0, \quad (29)$$

which on subtracting (29) from (28) yields $D_{-2}^2\phi_4 = 0$, hence

$$\phi_4(x, T_{-2}, T_{-1}, \dots) = 0. \quad (30)$$

Eq. (29) will be used later in the construction of our averaged equation.

The terms of the order of $\mathcal{O}(\epsilon^{1/2})$ give

$$D_{-2}^2\phi_5 + \alpha(D_{-2}\phi_3 + D_1\phi_0) + 2D_0D_1\phi_0 + \cos(\phi_0 + \theta)\phi_1 = 0, \quad (31)$$

with the solvability condition

$$2D_0D_1\phi_0 + \alpha D_1\phi_0 = 0. \quad (32)$$

Subtracting (32) from (31), we obtain

$$D_{-2}^2\phi_5 + \alpha D_{-2}\phi_3 + \cos(\phi_0 + \theta)\phi_1 = 0, \quad (33)$$

whose solution is

$$\phi_5(x, T_{-2}, \dots) = -F \cos(\phi_0 + \theta) \cos(T_{-2}) + \alpha^2 F \cos(T_{-2}). \quad (34)$$

The terms of order $\mathcal{O}(\epsilon)$ give

$$D_{-2}^2\phi_6 + 2D_{-2}D_{-1}\phi_5 + 2D_0D_2\phi_0 + D_1^2\phi_0 + \alpha D_2\phi_0 - \frac{1}{2}\phi_1^2 \sin(\phi_0 + \theta) = 0, \quad (35)$$

which gives the solvability condition

$$(2D_0D_2 + D_1^2)\phi_0 + \alpha D_2\phi_0 - \frac{1}{2}\langle\phi_1^2\rangle \sin(\phi_0 + \theta) = 0. \quad (36)$$

Subtracting (36) from (35), we obtain

$$D_{-2}^2\phi_6 + 2D_{-2}D_{-1}\phi_5 - \frac{1}{2}(\phi_1^2 - \langle\phi_1^2\rangle) \sin(\phi_0 + \theta) = 0. \quad (37)$$

In [9,30,31], a double sine-Gordon equation is obtained as the governing equation for the dynamics on the slow time scale. To obtain a similar equation for ϕ_0 , we need to proceed with the further calculations. Nevertheless, from hereon we are not going to calculate the explicit solutions of ϕ_j ($j \geq 6$) they contribute to higher-order corrections, we focus on finding the solvability conditions.

From the terms of order $\mathcal{O}(\epsilon^{3/2})$, we obtain

$$\begin{aligned} D_{-2}^2\phi_7 + 2D_{-2}D_{-1}\phi_6 + (2D_{-2}D_0 + D_{-1}^2)\phi_5 \\ + 2(D_0D_3 + D_1D_2)\phi_0 + \alpha(D_{-2}\phi_5 + D_3\phi_0) \\ + \cos(\phi_0 + \theta)\left(\phi_3 - \frac{1}{6}\phi_1^3\right) = 0, \end{aligned} \quad (38)$$

from which one obtains the solvability condition

$$2(D_0D_3 + D_1D_2)\phi_0 + \alpha D_3\phi_0 = 0. \quad (39)$$

The terms of order $\mathcal{O}(\epsilon^2)$ give

$$\begin{aligned} D_{-2}^2\phi_8 + 2D_{-2}D_{-1}\phi_7 + 2D_{-2}D_0\phi_6 + D_{-1}^2\phi_5 \\ + 2(D_{-2}D_1 + D_{-1}D_0)\phi_5 + 2(D_0D_4 + D_1D_3)\phi_0 \\ + D_2^2\phi_0 + \alpha(D_{-2}\phi_6 + D_{-1}\phi_5 + D_4\phi_0) \\ + \left(\frac{1}{24}\phi_1^4 - \phi_3\phi_1\right) \sin(\phi_0 + \theta) = 0. \end{aligned} \quad (40)$$

Using the Fredholm alternative, the solvability condition for the above equation is

$$\begin{aligned} D_2^2\phi_0 + (2D_0D_4 + 2D_1D_3)\phi_0 + \alpha D_4\phi_0 \\ + \frac{1}{24}\langle\phi_1^4\rangle \sin(\phi_0 + \theta) = 0. \end{aligned} \quad (41)$$

The terms of order $\mathcal{O}(\epsilon^{5/2})$ give

$$\begin{aligned} D_{-2}^2\phi_9 + 2D_{-2}D_{-1}\phi_8 + 2D_{-2}D_0\phi_7 + D_{-1}^2\phi_6 \\ + 2(D_{-2}D_1 + D_{-1}D_0)\phi_6 + 2(D_{-2}D_2 + D_{-1}D_1)\phi_5 \\ + D_0^2\phi_5 + 2(D_0D_5 + D_1D_4 + D_2D_3)\phi_0 \\ + \alpha(D_{-1}\phi_6 + D_0\phi_5 + D_{-2}\phi_7 + D_5\phi_0) + \cos(\phi_0 + \theta)\phi_5 \\ - \left(\frac{1}{2}\phi_3\phi_1^2 - \frac{1}{120}\phi_1^5\right) \cos(\phi_0 + \theta) = 0, \end{aligned} \quad (42)$$

which yields the solvability condition

$$2(D_0D_5 + D_1D_4 + D_2D_3)\phi_0 + \alpha D_5\phi_0 = 0. \quad (43)$$

Terms of order $\mathcal{O}(\epsilon^3)$ give

$$\begin{aligned} D_{-2}^2\phi_{10} + 2D_{-2}D_{-1}\phi_9 + 2D_{-2}D_0\phi_8 + D_{-1}^2\phi_7 \\ + 2(D_{-2}D_1 + D_{-1}D_0)\phi_7 + D_0^2\phi_6 \\ + 2(D_{-2}D_2 + D_{-1}D_1)\phi_6 \\ + 2(D_{-2}D_3 + D_{-1}D_2 + D_0D_1)\phi_5 + D_3^2\phi_0 \\ + 2(D_1D_5 + D_2D_4 + D_0D_6)\phi_0 \\ + \alpha(D_6\phi_0 + D_{-2}\phi_8 + D_{-1}\phi_7 + D_0\phi_6 + D_1\phi_5) \\ + \left(\frac{1}{6}\phi_3\phi_1^3 - \frac{1}{720}\phi_1^6 - \frac{1}{2}\phi_3^2 - \phi_5\phi_1\right) \sin(\phi_0 + \theta) \\ + \cos(\phi_0 + \theta)\phi_6 = 0, \end{aligned} \quad (44)$$

from which we obtain the solvability condition

$$\begin{aligned} D_3^2\phi_0 + 2(D_1D_5 + D_2D_4 + D_0D_6)\phi_0 + \alpha D_6\phi_0 \\ - \left(\langle\phi_5\phi_1\rangle + \frac{1}{720}\langle\phi_1^6\rangle + \frac{1}{2}\langle\phi_3^2\rangle\right) \sin(\phi_0 + \theta) = 0. \end{aligned} \quad (45)$$

We will not proceed further, as we have obtained a double-angle term in the average equation, through the terms $\langle\phi_5\phi_1\rangle$ (see (18) and (34)).

To obtain an average equation, we add Eqs. (21), (29), (32), (36), (39), (43), (41) and (45), and calculating the right hand side using averaging, thus

$$\begin{aligned} \frac{\partial^2\phi_0}{\partial t^2} - \frac{\partial^2\phi_0}{\partial x^2} + \alpha \frac{\partial\phi_0}{\partial t} - \gamma \\ = \left(\frac{\epsilon F^2}{4} - \frac{\epsilon^2 F^4}{64} + \frac{\epsilon^3 F^6}{2304} - \frac{\epsilon^3 \alpha^2 F^2}{4} - 1\right) \sin(\phi_0 + \theta) \\ + \frac{\epsilon^3 F^2}{4} \sin(2\phi_0 + 2\theta), \end{aligned} \quad (46)$$

reintroducing the original scaling (8), we obtain the ‘average’ equation, the double sine-Gordon equation

$$\begin{aligned} \frac{\partial^2\phi_0}{\partial x^2} - \frac{\partial^2\phi_0}{\partial t^2} - \alpha \frac{\partial\phi_0}{\partial t} + \gamma \\ = j_1 \sin(\phi_0 + \theta) - j_2 \sin(2\phi_0 + 2\theta), \end{aligned} \quad (47)$$

with

$$j_1 = 1 - \frac{f^2}{4\Omega^4} + \frac{f^4}{64\Omega^8} + \frac{\alpha^2 f^2}{4\Omega^6} - \frac{f^6}{2304\Omega^{12}} + \dots, \quad (48)$$

$$j_2 = \frac{f^2}{4\Omega^6} + \dots. \quad (49)$$

In [9,30,31], using different methods and for $\theta \equiv 0$, the coefficients j_i of the average equation above were given by

$$j_1 = J_0(a_1) + \frac{a_1^2 \alpha^2 (J_2(a_1) - J_0(a_1))}{4\Omega^2} + \frac{a_1 \alpha^2 J_1(a_1)}{\Omega^2}, \quad (50)$$

$$j_2 = \frac{J_1^2(a_1)}{\Omega^2} + \frac{a_1^2 \alpha^2 J_0(a_1)J_2(a_1)}{32\Omega^4} + \frac{a_1 \alpha^2 J_1(a_1)J_2(a_1)}{16\Omega^4}, \quad (51)$$

with $a_1 = -f/\Omega^2$ and J_i for $i = 0, 1, 2$ are Bessel functions of the first kind. One can confirm that (48) and (49) are the leading order series expansions of (50) and (51) via simple inspection.

3. Critical facet length and critical current in long Josephson junctions with phase-shifts

In this section, we discuss the effect of the oscillating drive to the ground state of Josephson junctions with phase-shifts $\theta(x)$ defined by (2) or (3).

3.1. $0 - \pi - 0$ junctions without dc-current

We consider first the case of $0 - \pi - 0$ junctions, i.e. $\theta(x)$ given by (2) in the absence of a constant bias current ($\gamma = 0$). Note that the length of the π region is also referred to as the facet length. The ground state of such a junction crucially depends on the parameter a . As mentioned above, there is a critical facet length a_c above which the ground state is nonuniform. Such a ground state represents an antiferromagnetically ordered semivortex–antisevivortex state [26].

One may calculate the critical facet length of the average Eq. (47) through calculating the value of a at which the zero

solution changes its stability. Using a simple calculation, one can obtain the linearized equation about $\phi_0 = 0$ of (47)

$$\phi_{1,xx} - \phi_{1,tt} = j_1 \cos(\theta)\phi_1 - 2j_2 \cos(2\theta)\phi_1, \quad (52)$$

whose solution can be easily calculated as

$$\phi_1(x, t) = B e^{i\omega t} \begin{cases} \cos(a\sqrt{j_1 - 2j_2 + \omega^2})e^{\sqrt{j_1 - 2j_2 - \omega^2}(a+x)}, & x < -a, \\ \cos(x\sqrt{j_1 - 2j_2 + \omega^2}), & |x| < a, \\ \cos(a\sqrt{j_1 - 2j_2 + \omega^2})e^{\sqrt{j_1 - 2j_2 - \omega^2}(a-x)}, & x > a. \end{cases} \quad (53)$$

The relation $a = a(\omega)$ is then given by

$$a = \frac{1}{\sqrt{j_1 - 2j_2 + \omega^2}} \tan^{-1} \left(\frac{\sqrt{j_1 - 2j_2 - \omega^2}}{\sqrt{j_1 - 2j_2 + \omega^2}} \right). \quad (54)$$

Half the critical facet length a_c is defined as the point where $\omega = 0$, that is,

$$a_c = \frac{\pi}{4\sqrt{j_1 - 2j_2}}. \quad (55)$$

As to leading order $j_2 \ll 1, j_1 = \mathcal{O}(1)$ and $j_1 < 1$, (55) implies that the ac-drive increases the critical facet length.

3.2. $0 - \kappa$ junctions with constant bias current

For the phase-shift configuration $\theta(x)$ given by (3), there is a critical bias current γ_c above which the junction has no static ground states. Here, we follow the calculation of, e.g., [34]. First, we rescale

$$x = \frac{\tilde{x}}{\sqrt{j_1}}, \quad \tilde{d} = -\frac{j_2}{j_1}, \quad \tilde{\gamma} = \frac{\gamma}{j_1}, \quad \tilde{\gamma}_c = \frac{\gamma_c}{j_1}. \quad (56)$$

With the above scalings, Eq. (47) becomes

$$\frac{\partial^2 \phi_0}{\partial \tilde{x}^2} = \sin(\phi_0 + \theta) + \tilde{d} \sin(2(\phi_0 + \theta)) - \tilde{\gamma}. \quad (57)$$

The critical bias current γ_c is obtained when all the conditions

$$\phi_0(0^+) = \phi_0(0^-), \quad \frac{\partial}{\partial \tilde{x}} \phi_0(0^+) = \frac{\partial}{\partial \tilde{x}} \phi_0(0^-), \quad (58)$$

$$\frac{\partial^2}{\partial \tilde{x}^2} \phi_0(0^+) = \frac{\partial^2}{\partial \tilde{x}^2} \phi_0(0^-),$$

are satisfied.

Next, we need to determine the equation for $\phi_{0\tilde{x}}$. The first integral of Eq. (57) is

$$\frac{1}{2} \left(\frac{\partial \phi_0}{\partial \tilde{x}} \right)^2 = -\cos(\phi_0 + \theta) - \frac{\tilde{d}}{2} \cos(2(\phi_0 + \theta)) - \tilde{\gamma} \phi_0 + C_{\pm}, \quad (59)$$

where C_{\pm} are constants of integration, i.e. C_+ for the region $\tilde{x} > 0$ and C_- for $\tilde{x} < 0$. The constants are obtained from the boundary conditions

$$\lim_{\tilde{x} \rightarrow \pm\infty} \phi_0(\tilde{x}) = \phi_{0\pm},$$

a consequence of this

$$\lim_{\tilde{x} \rightarrow \pm\infty} \phi_{0\tilde{x}}(\tilde{x}) = 0,$$

which correspond to kink solutions with nonzero constant drive. The integral constants C_{\pm} can then be calculated as

$$C_- = \cos(\phi_{0-}) + \frac{\tilde{d}}{2} \cos(2\phi_{0-}) + \tilde{\gamma} \phi_{0-}, \quad (60)$$

$$C_+ = \cos(\phi_{0+} - \kappa) + \frac{\tilde{d}}{2} \cos(2\phi_{0+} - \kappa) + \tilde{\gamma} \phi_{0+}. \quad (61)$$

Eqs. (57) and (59) and the conditions in (58) determine γ_c as a function of κ and \tilde{d} .

Rather than obtaining an explicit expression of γ for any \tilde{d} , here we calculate it perturbatively for small \tilde{d} , which is relevant for the scaling (8). Hence, we expand all quantities as follows

$$\phi_0 \approx \phi^{(0)} + \tilde{d} \phi^{(1)}, \quad \tilde{\gamma} \approx \tilde{\gamma}^{(0)} + \tilde{d} \tilde{\gamma}^{(1)}, \\ \tilde{\gamma}_c \approx \tilde{\gamma}_c^{(0)} + \tilde{d} \tilde{\gamma}_c^{(1)}.$$

Substituting these expansions into (57) and (59), equating the $\mathcal{O}(\tilde{d})$ terms we obtain the equations

$$\phi_{\tilde{x}\tilde{x}}^{(1)} = \begin{cases} \phi^{(1)} \cos(\phi^{(0)}) + \sin 2(\phi^{(0)}) - \tilde{\gamma}^{(1)}, & (\tilde{x} < 0), \\ \phi^{(1)} \cos(\phi^{(0)} - \kappa) + \sin 2(\phi^{(0)} - \kappa) - \tilde{\gamma}^{(1)}, & (\tilde{x} > 0), \end{cases} \quad (62)$$

$$\phi_{\tilde{x}}^{(0)} \phi_{\tilde{x}}^{(1)} = \begin{cases} \phi_-^{(1)} \sin(\phi_-^{(0)}) - \phi^{(1)} \sin(\phi^{(0)}) - \tilde{\gamma}^{(0)} (\phi^{(1)} - \phi_-^{(1)}) \\ \quad - \tilde{\gamma}^{(1)} (\phi^{(0)} - \phi_-^{(0)}) + \frac{1}{2} (\cos 2(\phi_-^{(0)})) \\ \quad - \cos 2(\phi^{(0)}), & (\tilde{x} < 0), \\ \phi_+^{(1)} \sin(\phi_+^{(0)} - \kappa) - \phi^{(1)} \sin(\phi^{(0)} - \kappa) \\ \quad - \tilde{\gamma}^{(0)} (\phi^{(1)} - \phi_+^{(1)}) - \tilde{\gamma}^{(1)} (\phi^{(0)} - \phi_+^{(0)}) \\ \quad + \frac{1}{2} (\cos 2(\phi_+^{(0)} - \kappa)) \\ \quad - \cos 2(\phi^{(0)} - \kappa), & (\tilde{x} > 0), \end{cases} \quad (63)$$

where

$$\phi_{\pm}^{(i)} = \lim_{\tilde{x} \rightarrow \pm\infty} \phi^{(i)}, \quad i = 0, 1.$$

We also conclude that

$$\phi_-^{(0)} = \arcsin \tilde{\gamma}^{(0)} = \phi_+^{(0)} - \kappa, \quad (64)$$

$$\phi_-^{(1)} = \phi_+^{(1)} = \frac{\tilde{\gamma}^{(1)}}{\sqrt{1 - \tilde{\gamma}^{(0)2}}}. \quad (65)$$

From the condition (cf. (58))

$$\lim_{\tilde{x} \rightarrow 0^+} \phi_{\tilde{x}\tilde{x}}^{(i)} = \lim_{\tilde{x} \rightarrow 0^-} \phi_{\tilde{x}\tilde{x}}^{(i)}, \quad i = 0, 1,$$

we obtain

$$\phi^{(0)}(0) = \frac{\kappa}{2} + \frac{\pi}{2}, \quad \phi^{(1)}(0) = -2 \cos(\kappa/2).$$

The terms in the expansion of the critical bias current at $\mathcal{O}(1)$ and $\mathcal{O}(\tilde{d})$ are then given respectively by

$$\tilde{\gamma}_c^{(0)} = -\frac{2 \sin(\kappa/2)}{\kappa}, \quad \tilde{\gamma}_c^{(1)} = 0, \quad (66)$$

i.e. the second harmonic does not influence the critical current. Hence, reversing the scaling (56) leading order the critical current is

$$\gamma_c = -\frac{2j_1 \sin(\kappa/2)}{\kappa}, \quad (67)$$

from which we obtain that the ac-drive term of amplitude f has the effect of reducing the critical bias current by an amount of $\mathcal{O}(f^2/\Omega^4)$.

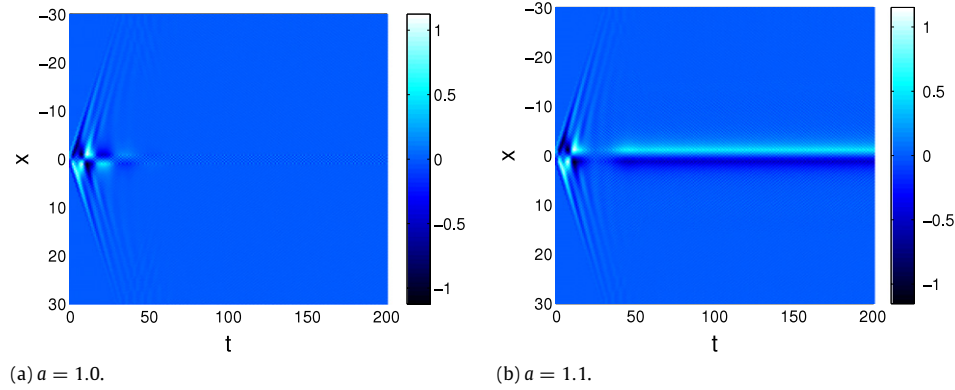


Fig. 1. We plot ϕ_x against (x, t) to illustrate the time dynamics of the phase-difference ϕ of (1) with θ given in (2), $f = 140$ and $\Omega = 10$. Half the facet length is depicted in the caption of each panel.

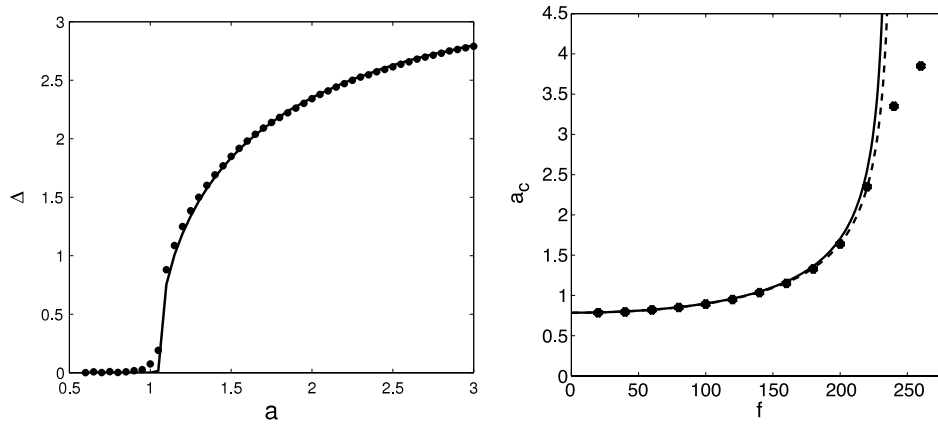


Fig. 2. The left panel shows the amplitude of the ground state Δ of the junction as a function of a . Filled circles are data from (1) and the solid line is from (47). The right panel depicts half the critical facet length a_c as a function of the oscillation amplitude f with $\Omega = 10$. Filled circles are data obtained from a numerical simulation of the governing Eq. (1) and the solid line is the analytical result (55) with j_i obtained using our method (48)–(49). The dashed line is the analytical result (55) with j_i from [30,31], i.e. (50)–(51).

4. Numerical results

Here, we compare the analytical results obtained in the preceding section with the numerics of the original governing Eq. (1). In all the results presented herein, we set $\alpha = 0.2$. We use periodic boundary conditions in a relatively long domain, i.e. $|x| < L$, $L \gg 1$ (particularly for $L = 100$), to simulate the infinite regime. The derivative with respect to x is approximated with either finite difference or spectral discretization with the spatial discretization $\delta x = 0.05$. The derivative with respect to t is integrated using a Runge–Kutta solver of fourth order using the temporal discretization $\delta t = 0.005$.

4.1. $0 - \pi - 0$ junctions without a constant bias current

First, we consider the ground state of $0 - \pi - 0$ junctions with $\gamma = 0$. In the absence of ac-drives ($f = 0$), when half the facet length a is larger than $\pi/4$, the uniform zero solution is unstable [26].

Fig. 1(a) shows the dynamics of the phase-difference $\phi(x, t)$ for $a = 1$. At $t = 0$, we use a zero initial displacement and velocity. With $f = 140$ and $\Omega = 10$, one notices that the zero solution is stable, even though $a > \pi/4$. Yet, when $a = 1.1$ it can be easily seen in Fig. 1(b) that the ground state is nonuniform. In the left panel of Fig. 2, we show the amplitude of the ground state Δ as a function of half the facet length a (filled circles). Because the background is rapidly oscillating due to the presence of the ac-drive, here we calculate Δ as the temporal average of the quantity $\delta\phi = \phi(0, t) - \phi(L, t)$ after the transient state disappears, which

is typically in the interval $100 < t < 200$. Half the critical facet length is the point where a solution with nonzero Δ bifurcates from the trivial solution ($\Delta = 0$ corresponds to uniform solution). From Fig. 1(a), one can deduce that the critical facet length is larger than $\pi/4$ for nonzero f . The solid line in the figure is the amplitude of the ground state Δ obtained from the average Eq. (47) with j_i given by (48)–(49). We see that (47) indeed approximates the slow time dynamics of (1).

Performing the same calculations at several values of f , one will obtain $a_c(f)$. The right panel of Fig. 2 shows the numerical results obtained from solving the governing Eq. (1). We also plot in the same figure (solid curve) the analytical approximation given by (55) with j_i given by (48)–(49), where good agreement is obtained. For completeness, we also plot the analytical approximation (55) with j_i given by (50)–(51). For $\Omega = 10$, one can note that the numerics deviates from the approximations at $f \approx 220$, i.e. near the singularity point when the denominator of (55) vanishes. From the numerics, it is clear that the singularity is only an artefact of the averaging and scaling we used. To capture this range of f , it is apparent that one needs a scaling beyond the threshold one mentioned above, i.e. $f = F/\epsilon^p$, where $p \geq 2$. The applicability of the method presented in this work in that case is suggested as future work.

4.2. $0 - \kappa$ junctions with constant bias current

Next, we study the effect of ac-drive to the critical bias current of a $0 - \kappa$ junction. Here, we only consider the case of $\kappa = \pi$, which

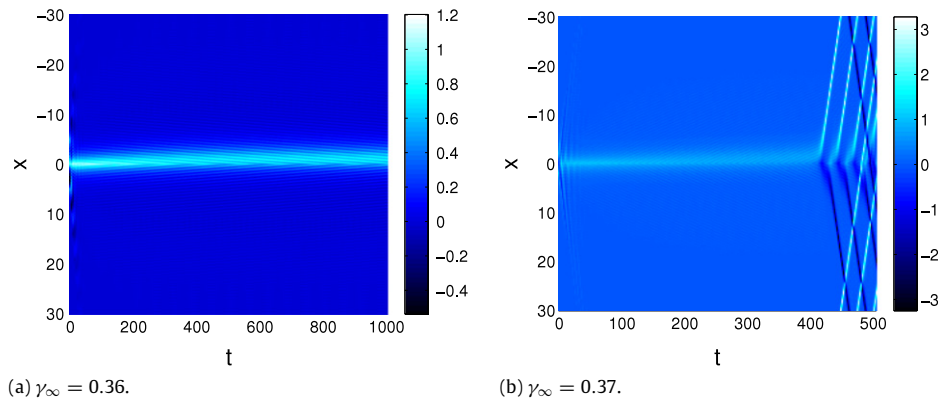


Fig. 3. We plot ϕ_x against (x, t) to illustrate the time dynamics of the phase-difference ϕ of (1) with θ given in (3), $f = 140$ and $\Omega = 10$. The constant bias current is depicted in the caption of each panel.

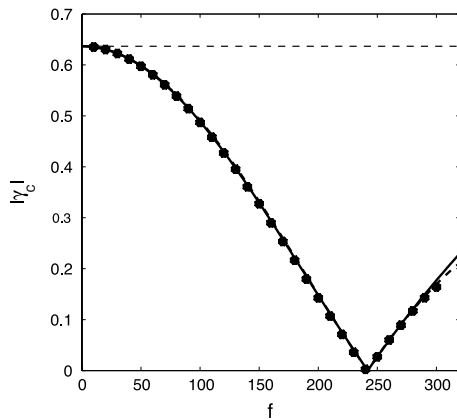


Fig. 4. Plot of the critical bias current density γ_c as a function of the forcing amplitude f , with $\Omega = 10$. Filled circles are data obtained from the governing Eq. (1) and the solid line is the analytical result (55) with j_i obtained using our method (48)–(49). The horizontal dashed line shows the critical bias current in the absence of ac-drives. The other dashed line is the analytical result (67) with j_i from [30,31], i.e. quantities (50)–(51).

is representative for this type of junction as the other values of κ can be calculated similarly.

In the absence of an ac-drive, it is known that when $\gamma > 2/\pi$, $0 - \pi$ junctions switch into a resistive state where at the point of the phase-shift, i.e. the discontinuity point, fluxons and antifluxons are periodically released [26,35–37]. Recall that for $\gamma = f = 0$, an exact solution of the ground state is given in (7).

Using numerical simulation to determine the critical bias current γ_c of Eq. (1) with $\theta(x)$ given in (3), one cannot immediately apply a fixed constant γ , as this will create shock and will switch the junction into nonzero voltage states. Because of that, in the simulation we slowly increases the bias current

$$\gamma = \gamma_\infty (1 - e^{-t/\tau}), \quad (68)$$

with $\tau = 100$. This choice of function allows the ground state to gradually adjust itself to the presence of the ac-drive. Larger values of τ have been tested as well and we did not see any prominent quantitative difference. At $t = 0$, the initial profile is an exact solution of the system with $f = 0$ and zero initial velocity.

In Fig. 3(a) we show a typical evolution of ϕ_x in the presence of an ac-drive with $f = 140$ and $\Omega = 10$ and an external bias current that is slowly increased to the value of $\gamma_\infty = 0.36$. One can notice that the nonuniform state is deformed due to the dc bias current and tends to a steady state in the limit $t \rightarrow \infty$.

In Fig. 3(b), we depict the dynamics of the variable ϕ_x when $\gamma_\infty = 0.37$. Here, we see a periodic release of fluxons and antifluxons indicating that the value of the bias current is above

the threshold value γ_c (see, e.g., [36,37]). It is important to note that $0.37 < 2/\pi$, i.e. the presence of $f \neq 0$ can indeed decrease the value of the critical bias current γ_c .

The critical bias current γ_c for different values of the driving amplitude f with $\Omega = 10$ is shown in Fig. 4, where the stars are data obtained numerically from (1) and the solid line is the analytical result (67) with j_i given by (48)–(49). We observe good agreement between the approximation and the numerics. Note that there is a threshold value of f at which the critical bias current vanishes, i.e. at $f \approx 240$. As the ac-driving amplitude is increased further, we obtain a situation where the numerical data deviates slightly from the approximation.

As a comparison, we also plot the analytical approximation (67) with j_i given by (50)–(51), we still obtain good agreement between numerics and the approximation. Hence, we argue that the deviation is due to the truncation error in (48)–(49), unlike the case in $0 - \pi - 0$ junctions in the previous section.

5. Conclusion

We have studied the dynamics of long Josephson junctions with phase-shifts in the presence of rapidly varying driving force. The ac-drive is assumed to be fast compared to the system's plasma frequency. We derived analytically an average equation for the slowly-varying dynamics. The obtained average equation is a double sine-Gordon equation. In particular, we obtained analytically the critical value of the applied constant bias current γ_c for the $0 - \kappa$ junctions and the critical facet length in the absence of external constant bias current for the $0 - \pi - 0$ junctions. Numerical computations have been performed, and good agreement was obtained.

References

- [1] A. Barone, G. Paterno, Physics and Applications of the Josephson Effect, John Wiley & Sons, New York, 1982.
- [2] K.K. Likharev, Dynamics of Josephson Junctions and Circuits, CRC Press, New York, 1986.
- [3] S. Shapiro, A.R. Janus, S. Holly, Rev. Modern Phys. 36 (1964) 223.
- [4] N.R. Quintero, A. Sánchez, Eur. Phys. J. B 6 (1998) 133–142.
- [5] S. Flach, Y. Zolotaryuk, A.E. Miroshnichenko, M.V. Fistul, Phys. Rev. Lett. 88 (2002) 184101.
- [6] E. Goldobin, B.A. Malomed, A.V. Ustinov, Phys. Rev. E 65 (2002) 056613.
- [7] M. Beck, E. Goldobin, M. Neuhaus, M. Siegel, R. Kleiner, D. Koelle, Phys. Rev. Lett. 95 (2005) 090603.
- [8] A.V. Ustinov, C. Coqui, A. Kemp, Y. Zolotaryuk, M. Salerno, Phys. Rev. Lett. 93 (2004) 087001.
- [9] V. Zharnitsky, I. Mitkov, N. Grønbech-Jensen, Phys. Rev. E 58 (1998) R52.
- [10] A.P. Itin, Phys. Rev. E 63 (2001) 028601.
- [11] J. Pfeiffer, M. Kemmler, D. Koelle, R. Kleiner, E. Goldobin, M. Weides, A.K. Feofanov, J. Lisenfeld, A.V. Ustinov, Phys. Rev. B 77 (2008) 214506.
- [12] K. Buckenmaier, T. Gaber, M. Siegel, D. Koelle, R. Kleiner, E. Goldobin, Phys. Rev. Lett. 98 (2007) 117006.

- [13] J. Pfeiffer, T. Gaber, D. Koelle, R. Kleiner, E. Goldobin, M. Weides, H. Kohlstedt, J. Lisenfeld, A.K. Feofanov, A.V. Ustinov, [arXiv:0903.1046](https://arxiv.org/abs/0903.1046), 2009.
- [14] M. Moshe, R.G. Mints, *Phys. Rev. B* 76 (2007) 054518.
- [15] L.N. Bulaevskii, V.V. Kuzii, A.A. Sobyenin, *Pis'ma Zh. Eksp. Teor. Fiz.* 25 (1977) 314; *JETP Lett.* 25 (1977) 290.
- [16] L.N. Bulaevskii, V.V. Kuzii, A.A. Sobyenin, *Solid State Commun.* 25 (1978) 1053.
- [17] O. Vávra, S. Gaži, D.S. Golubović, I. Vávra, J. Dérer, J. Verbeeck, G. Van Tendeloo, V.V. Moshchalkov, *Phys. Rev. B* 74 (2006) 020502.
- [18] T. Golod, A. Rydh, V.M. Krasnov, Detection of the phase shift from a single Abrikosov vortex, *Phys. Rev. Lett.* 104 (2010) 227003.
- [19] V.V. Ryazanov, V.A. Oboznov, A.Yu. Rusanov, A.V. Veretennikov, A.A. Golubov, J. Aarts, *Phys. Rev. Lett.* 86 (2001) 2427.
- [20] E. Goldobin, A. Sterck, T. Gaber, D. Koelle, R. Kleiner, *Phys. Rev. Lett.* 92 (2004) 057005.
- [21] C.C. Tsuei, J.R. Kirtley, *Rev. Modern Phys.* 72 (2000) 969.
- [22] H. Hilgenkamp, Ariando, H.-J.H. Smilde, D.H.A. Blank, G. Rijnders, H. Rogalla, J.R. Kirtley, C.C. Tsuei, *Nature* 422 (2003) 50.
- [23] A. Gumann, C. Iniotakis, N. Schopohl, *Appl. Phys. Lett.* 91 (2007) 192502.
- [24] C. Nappi, E. Sarnelli, M. Adamo, M.A. Navacerrada, *Phys. Rev. B* 74 (2006) 144504.
- [25] A. Ali, H. Susanto, J.A.D. Wattis, *SIAM J. Appl. Math.* 71 (2011) 242–269.
- [26] T. Kato, M. Imada, *J. Phys. Soc. Japan* 66 (1997) 1445.
- [27] S.M. Frolov, M.J.A. Stoutimore, T.A. Crane, D.J. Van Harlingen, V.A. Oboznov, V.V. Ryazanov, A. Ruosi, C. Granata, M. Russo, *Nat. Phys.* 4 (2008) 32–36.
- [28] B.A. Malomed, A.V. Ustinov, *Phys. Rev. B* 69 (2004) 064502.
- [29] E. Goldobin, N. Stefanakis, D. Koelle, R. Kleiner, *Phys. Rev. B* 70 (2004) 094520.
- [30] Yu.S. Kivshar, N. Grönbech-Jensen, R.D. Parmentier, *Phys. Rev. E* 49 (1994) 4542–4551.
- [31] Yu.S. Kivshar, K.H. Spatschek, *Chaos Solitons Fractals* 5 (1995) 2551–2569.
- [32] L.D. Landau, E.M. Lifshitz, *Mechanics*, Pergamon Press, New York, 1976.
- [33] V.I. Arnol'd, M. Levi, *Geometrical Methods in the Theory of Ordinary Differential Equations*, Springer-Verlag, 1988.
- [34] H. Susanto, S.A. van Gils, *Phys. Rev. B* 69 (2004) 092507.
- [35] A.B. Kuklov, V.S. Boyko, J. Malinsky, *Phys. Rev. B* 51 (1995) 11965–11968; *Phys. Rev. B* 55 (1997) 11878.
- [36] N. Stefanakis, *Phys. Rev. B* 66 (2002) 214524.
- [37] E. Goldobin, D. Koelle, R. Kleiner, *Phys. Rev. B* 67 (2003) 224515.